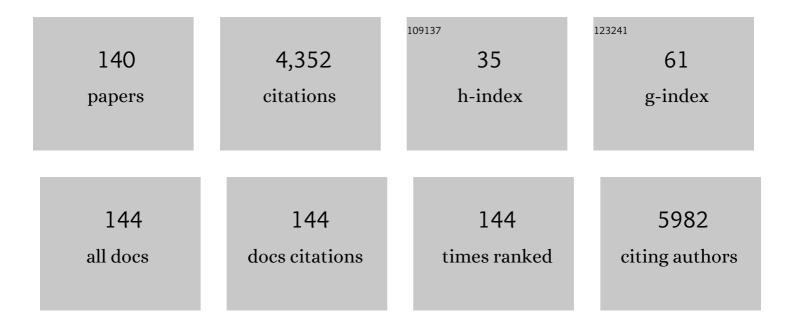
List of Publications by Year in descending order

Source: https://exaly.com/author-pdf/2677861/publications.pdf Version: 2024-02-01



SHIRINTI

#	Article	IF	CITATIONS
1	Dual-functional passivators for highly efficient and hydrophobic FA-based perovskite solar cells. Chemical Engineering Journal, 2022, 433, 133227.	6.6	11
2	Enhanced photovoltaic performance of SnO2 based flexible perovskite solar cells via introducing interfacial dipolar layer and defect passivation. Journal of Power Sources, 2022, 519, 230814.	4.0	8
3	Regulating crystallization dynamics and crystal orientation of methylammonium tin iodide enables high-efficiency lead-free perovskite solar cells. Nanoscale, 2022, 14, 1219-1225.	2.8	14
4	Zwitterion-Assisted Crystal Growth of 2D Perovskites with Unfavorable Phase Suppression for High-Performance Solar Cells. ACS Applied Materials & Interfaces, 2022, 14, 814-825.	4.0	7
5	Self-Powered All-Inorganic Perovskite Photodetectors with Fast Response Speed. Nanoscale Research Letters, 2021, 16, 6.	3.1	17
6	Efficient Stabilization and Passivation for Low-Temperature-Processed γ-CsPbI3 Solar Cells. ACS Applied Materials & Interfaces, 2021, 13, 18784-18791.	4.0	11
7	Antisolvent engineering for mixed tin-lead inorganic perovskite solar cells. Journal of Physics: Conference Series, 2021, 2011, 012094.	0.3	0
8	Targeted Distribution of Passivator for Polycrystalline Perovskite Light-Emitting Diodes with High Efficiency. ACS Energy Letters, 2021, 6, 4187-4194.	8.8	41
9	Unveiling the guest effect of N-butylammonium iodide towards efficient and stable 2D-3D perovskite solar cells through sequential deposition process. Chemical Engineering Journal, 2020, 391, 123589.	6.6	34
10	Flexible optoelectronic devices based on metal halide perovskites. Nano Research, 2020, 13, 1997-2018.	5.8	52
11	Synergistic effect of additives on 2D perovskite film towards efficient and stable solar cell. Chemical Engineering Journal, 2020, 389, 124266.	6.6	50
12	Large organic cation incorporation induces vertical orientation growth of Sn-based perovskites for high efficiency solar cells. Chemical Engineering Journal, 2020, 402, 125133.	6.6	25
13	Vacancies substitution induced interfacial dipole formation and defect passivation for highly stable perovskite solar cells. Chemical Engineering Journal, 2020, 396, 125010.	6.6	19
14	Mediator–Antisolvent Strategy to Stabilize All-Inorganic CsPbI <sub>3</sub> for Perovskite Solar Cells with Efficiency Exceeding 16%. ACS Energy Letters, 2020, 5, 1619-1627.	8.8	46
15	Controllable Two-dimensional Perovskite Crystallization via Water Additive for High-performance Solar Cells. Nanoscale Research Letters, 2020, 15, 108.	3.1	9
16	Mini Review on Flexible and Wearable Electronics for Monitoring Human Health Information. Nanoscale Research Letters, 2019, 14, 263.	3.1	172
17	Enhanced Electrons Extraction of Lithium-Doped SnO\$_{2}\$ Nanoparticles for Efficient Planar Perovskite Solar Cells. IEEE Journal of Photovoltaics, 2019, 9, 1273-1279.	1.5	10
18	High-Performance Paper-Based Capacitive Flexible Pressure Sensor and Its Application in Human-Related Measurement. Nanoscale Research Letters, 2019, 14, 183.	3.1	40

#	Article	IF	CITATIONS
19	Solution-Processed Inorganic Perovskite Flexible Photodetectors with High Performance. Nanoscale Research Letters, 2019, 14, 284.	3.1	21
20	Improved crystallinity of perovskite via molecularly tailored surface modification of SnO2. Journal of Power Sources, 2019, 441, 227161.	4.0	20
21	Enhanced thermal stability of electron transport layer-free perovskite solar cells via interface strain releasing. Journal of Power Sources, 2019, 439, 227091.	4.0	21
22	Low-temperature processed inorganic perovskites for flexible detectors with a broadband photoresponse. Nanoscale, 2019, 11, 2871-2877.	2.8	74
23	Flexible, UV-responsive perovskite photodetectors with low driving voltage. Journal of Materials Science, 2019, 54, 11556-11563.	1.7	17
24	Corrosive Behavior of Silver Electrode in Inverted Perovskite Solar Cells Based on Cu:NiO <sub>x</sub> . IEEE Journal of Photovoltaics, 2019, 9, 1081-1085.	1.5	17
25	Optimization of anti-solvent engineering toward high performance perovskite solar cells. Journal of Materials Research, 2019, 34, 2416-2424.	1.2	32
26	Steering the crystallization of perovskites for high-performance solar cells in ambient air. Journal of Materials Chemistry A, 2019, 7, 12166-12175.	5.2	65
27	Band alignment of Pb–Sn mixed triple cation perovskites for inverted solar cells with negligible hysteresis. Journal of Materials Chemistry A, 2019, 7, 9154-9162.	5.2	54
28	Enhanced performance of ZnO nanoparticle decorated all-inorganic CsPbBr <sub>3</sub> quantum dot photodetectors. Journal of Materials Chemistry A, 2019, 7, 6134-6142.	5.2	64
29	Enhanced Crystallinity of Triple-Cation Perovskite Film via Doping NH4SCN. Nanoscale Research Letters, 2019, 14, 304.	3.1	14
30	Strategies to Fabricate Flexible SnO2 Based Perovskite Solar Cells Using Pre-Crystallized SnO2. Journal of Physics: Conference Series, 2019, 1346, 012036.	0.3	0
31	To Reveal Grain Boundary Induced Thermal Instability of Perovskite Semiconductor Thin Films for Photovoltaic Devices. IEEE Journal of Photovoltaics, 2019, 9, 207-213.	1.5	10
32	Improved stability of perovskite solar cells with enhanced moisture-resistant hole transport layers. Electrochimica Acta, 2019, 296, 508-516.	2.6	17
33	Physisorption of Oxygen in SnO <sub>2</sub> Nanoparticles for Perovskite Solar Cells. IEEE Journal of Photovoltaics, 2019, 9, 200-206.	1.5	12
34	SnO <sub>2</sub> â€Based Perovskite Solar Cells: Configuration Design and Performance Improvement. Solar Rrl, 2019, 3, 1800292.	3.1	80
35	Humidity-insensitive fabrication of efficient perovskite solar cells in ambient air. Journal of Power Sources, 2019, 412, 359-365.	4.0	19
36	Solution processed PCBM-CH3NH3PbI3 heterojunction photodetectors with enhanced performance and stability. Organic Electronics, 2018, 57, 263-268.	1.4	28

#	Article	IF	CITATIONS
37	High Speed and Stable Solutionâ€Processed Triple Cation Perovskite Photodetectors. Advanced Optical Materials, 2018, 6, 1701341.	3.6	69
38	Theoretical lifetime extraction and experimental demonstration of stable cesium-containing tri-cation perovskite solar cells with high efficiency. Electrochimica Acta, 2018, 265, 98-106.	2.6	36
39	Perovskite Solar Cells with ZnO Electronâ€Transporting Materials. Advanced Materials, 2018, 30, 1703737.	11.1	319
40	Suppressed Decomposition of Perovskite Film on ZnO Via a Selfâ€Assembly Monolayer of Methoxysilane. Solar Rrl, 2018, 2, 1800240.	3.1	18
41	Strain relaxation in GaN/AlN superlattices on GaN(0001) substrate: Combined superlattice-to-substrate lattice misfit and thickness-dependent effects. Materials and Design, 2018, 157, 141-150.	3.3	5
42	Review Application of Nanostructured Black Silicon. Nanoscale Research Letters, 2018, 13, 110.	3.1	96
43	Reveal the growth mechanism in perovskite films via weakly coordinating solvent annealing. Science China Materials, 2018, 61, 1536-1548.	3.5	11
44	Photovoltaic Performance of Lead-Iodide Perovskite Solar Cells Fabricated Under Ambient Air Conditions With HTM Solution Excluding LiTFSI. IEEE Journal of Photovoltaics, 2018, 8, 1051-1057.	1.5	4
45	Highly sensitive and stable flexible pressure sensors with micro-structured electrodes. Journal of Alloys and Compounds, 2017, 699, 824-831.	2.8	49
46	Mesoporous PbI2 assisted growth of large perovskite grains for efficient perovskite solar cells based on ZnO nanorods. Journal of Power Sources, 2017, 342, 990-997.	4.0	105
47	Broadband infrared response of sulfur hyperdoped silicon under femtosecond laser irradiation. Materials Letters, 2017, 196, 16-19.	1.3	13
48	Highly sensitive hydrogen sensor based on Pd-functionalized titania nanotubes prepared in water-contained electrolyte. Journal of Materials Science: Materials in Electronics, 2017, 28, 1428-1432.	1.1	4
49	Realizing Full Coverage of Stable Perovskite Film by Modified Anti-Solvent Process. Nanoscale Research Letters, 2017, 12, 367.	3.1	18
50	Electronic Properties of a New All-Inorganic Perovskite TIPbI3 Simulated by the First Principles. Nanoscale Research Letters, 2017, 12, 232.	3.1	11
51	Enhanced Performance of Planar Perovskite Solar Cells Using Low-Temperature Solution-Processed Al-Doped SnO2 as Electron Transport Layers. Nanoscale Research Letters, 2017, 12, 238.	3.1	66
52	Interface engineering of high efficiency perovskite solar cells based on ZnO nanorods using atomic layer deposition. Nano Research, 2017, 10, 1092-1103.	5.8	134
53	Effect of well/barrier thickness ratio on strain relaxation in GaN/AlN superlattices grown on GaN/sapphire template. Journal of Vacuum Science and Technology B:Nanotechnology and Microelectronics, 2017, 35, .	0.6	5
54	Optical and structural study of deformation states in the GaN/AlN superlattices. Journal of Applied Physics, 2017, 122, .	1.1	11

#	Article	IF	CITATIONS
55	Enhanced electronic transport in Fe <sup>3+</sup> -doped TiO <sub>2</sub> for high efficiency perovskite solar cells. Journal of Materials Chemistry C, 2017, 5, 10754-10760.	2.7	80
56	Enhanced efficiency and environmental stability of planar perovskite solar cells by suppressing photocatalytic decomposition. Journal of Materials Chemistry A, 2017, 5, 17368-17378.	5.2	72
57	Stitching triple cation perovskite by a mixed anti-solvent process for high performance perovskite solar cells. Nano Energy, 2017, 39, 616-625.	8.2	194
58	Controllable preparation of TiO <sub>2</sub> nanotube arrays on Ti foil substrates. Integrated Ferroelectrics, 2017, 182, 127-133.	0.3	1
59	Efficient planar heterojunction perovskite solar cells with Li-doped compact TiO 2 layer. Nano Energy, 2017, 31, 462-468.	8.2	244
60	Optical and Electronic Properties of Femtosecond Laser-Induced Sulfur-Hyperdoped Silicon N+/P Photodiodes. Nanoscale Research Letters, 2017, 12, 522.	3.1	18
61	Comprehensive study of the two-step solution processes in ambient air for lead iodide perovskite solar cells. , 2016, , .		1
62	(Invited) The Defects of ZnO Nanorods Passivated By Ultra-Thin Al <sub>2</sub> O <sub>3</sub> Film. ECS Transactions, 2016, 72, 275-285.	0.3	4
63	The Peculiarities of Strain Relaxation in GaN/AlN Superlattices Grown on Vicinal GaN (0001) Substrate: Comparative XRD and AFM Study. Nanoscale Research Letters, 2016, 11, 252.	3.1	12
64	Se doping of silicon with Si/Se bilayer films prepared by femtosecond-laser irradiation. Materials Science in Semiconductor Processing, 2016, 54, 51-56.	1.9	15
65	Pore-widening treatment-enhanced hydrogen sensing with nanoporous palladium films. , 2016, , .		1
66	High near infrared absorption of hyperâ€doped silicon induced by coâ€doping of sulfur and nitrogen. Physica Status Solidi (A) Applications and Materials Science, 2016, 213, 2855-2860.	0.8	3
67	Solvent annealing of PbI <sub>2</sub> for the high-quality crystallization of perovskite films for solar cells with efficiencies exceeding 18%. Nanoscale, 2016, 8, 19654-19661.	2.8	82
68	Semiconductor-metal phase transition properties and growth texture of vanadium dioxide films on Si <sub>3</sub> N <sub>4</sub> layer. Integrated Ferroelectrics, 2016, 171, 208-214.	0.3	0
69	Room-temperature and fast response hydrogen sensor based on annealed nanoporous palladium film. Journal of Materials Science, 2016, 51, 2420-2426.	1.7	21
70	Fast response hydrogen sensors based on anodic aluminum oxide with pore-widening treatment. Applied Surface Science, 2016, 380, 47-51.	3.1	16
71	The preparation and electrochemical properties of PEDOT:PSS/MnO2/PEDOT ternary film and its application in flexible micro-supercapacitor. Electrochimica Acta, 2016, 193, 199-205.	2.6	48
72	A modified sequential deposition method for fabrication of perovskite solar cells. Solar Energy, 2016, 126, 243-251.	2.9	38

#	Article	IF	CITATIONS
73	Enhanced electrochemical performance of laser scribed graphene films decorated with manganese dioxide nanoparticles. Journal of Materials Science: Materials in Electronics, 2016, 27, 2564-2573.	1.1	34
74	First-principles calculations of properties for chalcogen (S, Se, Te) doped silicon. Solid State Communications, 2016, 226, 1-4.	0.9	8
75	High responsivity of pyroelectric infrared detector based on ultra-thin (10Âμm) LiTaO3. Journal of Materials Science: Materials in Electronics, 2015, 26, 5400-5404.	1.1	17
76	Flexible conducting polymer/reduced graphene oxide films: synthesis, characterization, and electrochemical performance. Nanoscale Research Letters, 2015, 10, 222.	3.1	59
77	High-quality self-ordered TiO2 nanotubes on fluorine-doped tin oxide glass. Journal of Materials Science: Materials in Electronics, 2015, 26, 7081-7085.	1.1	9
78	Porous conducting polymer and reduced graphene oxide: preparation, characterization and electrochemical performance. Journal of Materials Science: Materials in Electronics, 2015, 26, 1668-1677.	1.1	14
79	Manganese dioxide nanoparticle enrichment in porous conducting polymer as high performance supercapacitor electrode materials. Electrochimica Acta, 2015, 165, 323-329.	2.6	49
80	PEDOT:PSS/graphene/PEDOT ternary film for high performance electrochemical electrode. Journal of Materials Science: Materials in Electronics, 2015, 26, 8292-8300.	1.1	22
81	A modified sequential method used to prepare high quality perovskite on ZnO nanorods. Chemical Physics Letters, 2015, 639, 283-288.	1.2	26
82	Near-infrared optical absorption enhanced in black silicon via Ag nanoparticle-induced localized surface plasmon. Nanoscale Research Letters, 2014, 9, 519.	3.1	35
83	Ordered and ultrathin reduced graphene oxide LB films as hole injection layers for organic light-emitting diode. Nanoscale Research Letters, 2014, 9, 537.	3.1	38
84	Study of a New Sol-Gel Spin-Coating Technology and Thermal-Resistance Properties for Vanadium Oxide Thin Films. Integrated Ferroelectrics, 2014, 153, 126-132.	0.3	2
85	Atomic Layer Deposition of High Quality HfO <sub>2</sub> Using In-Situ Formed Hydrophilic Oxide as an Interfacial Layer. ECS Journal of Solid State Science and Technology, 2014, 3, N155-N160.	0.9	2
86	Preparation and characteristics of vanadium oxide thin films by controlling the sputtering voltage. Optical Materials, 2014, 36, 1419-1423.	1.7	6
87	Influence of two-tier structuring on the performance of black silicon-based MSM photodetectors. Journal of Materials Science: Materials in Electronics, 2014, 25, 1542-1546.	1.1	2
88	Conducting polymer and reduced graphene oxide Langmuir–Blodgett films: a hybrid nanostructure for high performance electrode applications. Journal of Materials Science: Materials in Electronics, 2014, 25, 1063-1071.	1.1	25
89	Porous conducting polymer and reduced graphene oxide nanocomposites for room temperature gas detection. RSC Advances, 2014, 4, 42546-42553.	1.7	40
90	In Situ Polymerization Deposition of Porous Conducting Polymer on Reduced Graphene Oxide for Gas Sensor. ACS Applied Materials & Interfaces, 2014, 6, 13807-13814.	4.0	145

#	Article	IF	CITATIONS
91	Absorption enhancement of near infrared in Te doped nanoporous silicon. Journal of Materials Science: Materials in Electronics, 2013, 24, 2197-2201.	1.1	5
92	Electrochemical performance of conducting polymer and its nanocomposites prepared by chemical vapor phase polymerization method. Journal of Materials Science: Materials in Electronics, 2013, 24, 2245-2253.	1.1	25
93	Investigation of nanostructured silicon as a candidate for heat sensitive material. Journal of Materials Science: Materials in Electronics, 2013, 24, 1770-1774.	1.1	5
94	Chemical vapor phase polymerization deposition of layer-ordered conducting polymer nanostructure for hole injection layer. Journal of Materials Science: Materials in Electronics, 2013, 24, 1382-1388.	1.1	4
95	Electrical and optical properties of reactive sputtered TiO x thin films for uncooled IR detector applications. Journal of Materials Science: Materials in Electronics, 2013, 24, 1292-1297.	1.1	1
96	Electrochemical performance of graphene-polyethylenedioxythiophene nanocomposites. Materials Science and Engineering B: Solid-State Materials for Advanced Technology, 2013, 178, 1152-1157.	1.7	25
97	Sputtering Voltage in the Growth of Vanadium Oxide Thin Films. Integrated Ferroelectrics, 2013, 144, 154-160.	0.3	1
98	Black silicon with self-cleaning surface prepared by wetting processes. Nanoscale Research Letters, 2013, 8, 351.	3.1	33
99	Mechanism of optical absorption enhancement of surface textured black silicon. Journal of Materials Science: Materials in Electronics, 2013, 24, 463-466.	1.1	21
100	Transition of dominative conduction mechanism caused by nanostructures on silicon surface. Materials Letters, 2013, 94, 27-29.	1.3	1
101	Effects of rapid thermal annealing on the optical properties of strain-free quantum ring solar cells. Nanoscale Research Letters, 2013, 8, 5.	3.1	21
102	Vapor Phase Polymerization Deposition of Conducting Polymer/Graphene Nanocomposites as High Performance Electrode Materials. ACS Applied Materials & Interfaces, 2013, 5, 4350-4355.	4.0	36
103	Polarization induced hole doping in graded Al <i>x</i> Ga1â^' <i>x</i> N ( <i>x</i> = 0.7 â^¼â€‰1) la molecular beam epitaxy. Applied Physics Letters, 2013, 102, .	yer grown 1.5	by 74
104	Vapor Phase Polymerization Deposition Conducting Polymer Nanocomposites on Porous Dielectric Surface as High Performance Electrode Materials. Nano-Micro Letters, 2013, 5, 40-46.	14.4	20
105	High responsivity MSM black silicon photodetector. Materials Science in Semiconductor Processing, 2013, 16, 619-624.	1.9	29
106	Enhanced ultraviolet to near-infrared absorption by two-tier structured silicon formed by simple chemical etching. Philosophical Magazine, 2012, 92, 4291-4299.	0.7	6
107	Polarization doping: Reservoir effects of the substrate in AlGaN graded layers. Journal of Applied Physics, 2012, 112, 053711.	1.1	29
108	Ordered SrTiO3 Nanoripples Induced by Focused Ion Beam. Nano-Micro Letters, 2012, 4, 243-246.	14.4	3

#	Article	IF	CITATIONS
109	Silicon nanowires prepared by electron beam evaporation in ultrahigh vacuum. Nanoscale Research Letters, 2012, 7, 243.	3.1	9
110	Polarization induced pn-junction without dopant in graded AlGaN coherently strained on GaN. Applied Physics Letters, 2012, 101, .	1.5	114
111	Strain-free ring-shaped nanostructures by droplet epitaxy for photovoltaic application. Applied Physics Letters, 2012, 101, 043904.	1.5	57
112	Thermal etching process of microscale pits on the GaAs(001) surface. Physica Status Solidi - Rapid Research Letters, 2012, 6, 25-27.	1.2	8
113	Influence of Ga coverage on the sizes of GaAs quantum dash pairs grown by high temperature droplet epitaxy. Physica Status Solidi - Rapid Research Letters, 2012, 6, 309-311.	1.2	3
114	Heat sensitive property of sputtered titanium oxide thin films for uncooled IR detector application. Journal of Materials Science: Materials in Electronics, 2012, 23, 1188-1192.	1.1	10
115	Optical properties of black silicon prepared by wet etching. Journal of Materials Science: Materials in Electronics, 2012, 23, 1558-1561.	1.1	16
116	Enhancement of thermal conductivity of hydrogenated silicon film by microcrystalline structure growth. Journal of Materials Science: Materials in Electronics, 2012, 23, 224-228.	1.1	0
117	Low Temperature Fabrication of Nanostructured Titanium Oxide Thin Films for Uncooled IR Detectors. Journal of Nanoelectronics and Optoelectronics, 2012, 7, 317-321.	0.1	0
118	Organic Thin-Film Transistors Gas Sensor Based on Highly Compact and Ordered Phthalocyanine Semiconducting Nanofilms. Journal of Nanoelectronics and Optoelectronics, 2012, 7, 265-270.	0.1	0
119	Near infrared broadband emission of In0.35Ga0.65As quantum dots on high index GaAs surfaces. Nanoscale, 2011, 3, 1485.	2.8	12
120	Nanoscale Footprints of Self-Running Gallium Droplets on GaAs Surface. PLoS ONE, 2011, 6, e20765.	1.1	19
121	Insight into optical properties of strain-free quantum dot pairs. Journal of Nanoparticle Research, 2011, 13, 947-952.	0.8	7
122	Origins of 1/f noise in nanostructure inclusion polymorphous silicon films. Nanoscale Research Letters, 2011, 6, 281.	3.1	30
123	Polarization induced doping in graded AlGaN films. Physica Status Solidi C: Current Topics in Solid State Physics, 2011, 8, 2182-2184.	0.8	17
124	Effect of structure variation on thermal conductivity of hydrogenated silicon film. Applied Surface Science, 2011, 257, 8326-8329.	3.1	5
125	Formation of GaAs Double Rings Through Gallium Migration and Nanodrilling. Journal of Nanoelectronics and Optoelectronics, 2011, 6, 58-61.	0.1	5
126	Surface mediated control of droplet density and morphology on GaAs and AlAs surfaces. Physica Status Solidi - Rapid Research Letters, 2010, 4, 371-373.	1.2	12

#	Article	IF	CITATIONS
127	InGaAs Quantum Well Grown on High-Index Surfaces for Superluminescent Diode Applications. Nanoscale Research Letters, 2010, 5, 1079-1084.	3.1	23
128	Effect of the Chemical Oxide Layer Thickness on the Interfacial Quality of ALD-Grown HfO <sub>2</sub> on Silicon. ECS Transactions, 2010, 28, 89-95.	0.3	0
129	The Interfacial Quality of HfO[sub 2] on Silicon with Different Thicknesses of the Chemical Oxide Interfacial Layer. Journal of the Electrochemical Society, 2010, 157, G221.	1.3	17
130	Optical Absorption of Proton Irradiated Colloidal CdSe/ZnS Core/Shell Nanocrystals. IEEE Transactions on Nuclear Science, 2010, 57, 2929-2932.	1.2	1
131	Intersublevel Infrared Photodetector with Strain-Free GaAs Quantum Dot Pairs Grown by High-Temperature Droplet Epitaxy. Nano Letters, 2010, 10, 1512-1516.	4.5	116
132	Raman and ellipsometric characterization of hydrogenated amorphous silicon thin films. Science in China Series D: Earth Sciences, 2009, 52, 339-343.	0.9	4
133	Depth profile study on Raman spectra of high-energy-electron-irradiated hydrogenated amorphous silicon films. Science in China Series D: Earth Sciences, 2009, 52, 2406-2411.	0.9	1
134	Noise in boron doped amorphous/microcrystallization silicon films. Applied Surface Science, 2008, 254, 3274-3276.	3.1	5
135	Influence of substrate temperature on the microstructure and optical properties of hydrogenated silicon thin film prepared with pure silane. Physica B: Condensed Matter, 2008, 403, 2282-2287.	1.3	5
136	Growth mechanism of microcrystalline and polymorphous silicon film with pure silane source gas. Journal Physics D: Applied Physics, 2008, 41, 105207.	1.3	11
137	Effects of irradiation with electrons of different energies on the dark conductivity and the network of hydrogenated amorphous silicon films. Philosophical Magazine Letters, 2008, 88, 871-877.	0.5	3
138	Electron irradiation effects on the properties of heavily phosphorus-doped a-Si : H films prepared from undiluted silane. Journal Physics D: Applied Physics, 2008, 41, 205412.	1.3	8
139	Manufacturing and photoelectrical properties of P-doped a-Si:H thin films deposited by PECVD. , 2007, ,		0
140	Influence of microcrystallization on noise in boronâ€doped silicon film. Physica Status Solidi (A) Applications and Materials Science, 2007, 204, 4292-4297.	0.8	3